

# Simulation of spatio-temporal chaos in a Newton's Cradle, as a basis for development of an agent-based model for impacting mechanical systems

M. Charalambides<sup>1</sup> & D. J. Jefferies<sup>2</sup>

<sup>1,2</sup> Department of Electronic and Electrical Engineering, University of Surrey,  
Guildford GU2 5XH, Surrey, U.K.

Email: {eem1mc, d.jefferies}@eim.surrey.ac.uk

## Abstract

A model was used to study the chaotic behaviour of a five mass Newton's cradle arrangement. This system consists of an oscillating wall and five pendula, which are separated by a distance. The wall is able to drive the system by providing sufficient energy after colliding with the first pendulum. All the bodies are able to oscillate in the same vertical plane about their mean position, with the possibility of a collision.

The C programming language was utilized to investigate the behaviour of the system with all its complexities. Several filters were designed to extract the necessary parameters that describe the system and numerous simulations involving combinations of pendula were performed. The case of a single driven pendulum revealed very structured fractal geometry, while the five-pendulum system exhibited spatio-temporal chaos.

While this paper is not directly concerned with agent-based modelling of this system, it shows results that an agent-based model might also reveal. We are currently working on such an agent-based model for a two-dimensional array of impacting pendula, such as might for example represent the vibrating fuel rods in a nuclear reactor. It is clear that as the complexity of the problem increases, agent-based solutions become more computationally tractable, and possibly more computationally efficient.

## 1 Introduction

The aim is to model a five mass Newton's cradle arrangement and study its chaotic behaviour. The system consists of a rigid oscillating wall at one end that drives five pendula separated by a distance. The particles move in a vertical plane under the force of gravity. Furthermore, the presence of a damping factor influences the motion, making the system more realistic. The wall can provide energy upon collision with the first pendulum. Subsequent collisions among the pendula transfer the energy across the system.

In order to reach the point where chaos can be considered, the dynamics of the system need to be studied and analysed mathematically as to allow effective modelling. The first step will be to create and verify a consistent model that describes the motion of the system elements in time. Upon verification, the work will have to be extended and seek towards chaos. This will be achieved with the aid of several tools, specially designed to reveal the chaotic nature of dynamical systems.

Ordinarily, the system itself will only be a model of real world phenomena: certain assumptions will

be made, and certain approximations and experimental errors will be present. Hence the dynamical system itself, albeit a completely accurate solution of the physical model, will never the less be only an approximation to reality since the model itself suffers this flaw.

## 2 System Analysis - Dynamics

This section deals with the presentation of the system to be modelled, towards an effort to introduce the reader to the concept of an impacting system.

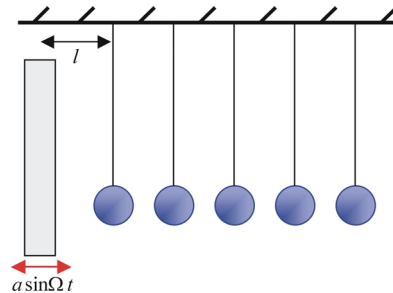


Figure 1. The proposed system

The aim is to analyse the system using simple

dynamics as to formulate it mathematically, taking into account all its complexities.

The system consists of five pendula and a wall (positioned at the left of the first pendulum), all separated by a distance  $l$ , as in figure 1.

## 2.1 The simple pendulum

Consider a pendulum bob,  $P$ , of mass  $m$  attached to a light inextensible string of length  $L$ . Suppose that the pendulum is suspended from a fixed point  $O$ , and that when the string is at an angle  $\vartheta$  to the vertical, the velocity of the bob is  $v$  (Fig. 2). The forces acting on the bob are its weight  $mg$ , and the tension  $T$  in the string.

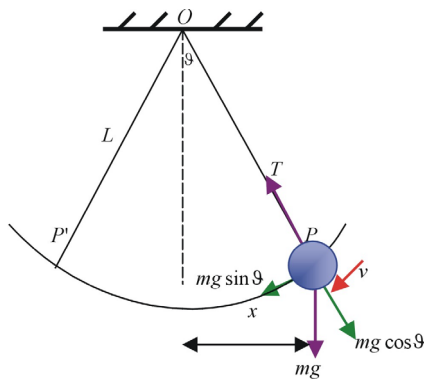


Figure 2. The simple pendulum

Resolving force  $mg$  into its components gives:

1.  $mg \cos \vartheta$  - parallel to  $OP$
2.  $mg \sin \vartheta$  - perpendicular to  $OP$

The second component is responsible for the oscillation of the system. Therefore, the force that preserves the oscillation is:

$$F = -mg \sin \vartheta \quad [2.1]$$

The negative sign accounts for the fact that the force tends to bring the bob back to equilibrium position. If we assume that the amplitude of oscillation is small,  $\vartheta$  is small and therefore the arc of oscillation can be approximated by the straight line  $PP'$ . Since:

$$\sin \vartheta = \frac{x}{L} \quad [2.2]$$

, then substituting in equation [2.1]:

$$F = -\left(\frac{mg}{L}\right)x \quad [2.3]$$

According to Muncaster R. (1993), it can be shown that the period of the bob oscillating with approximated simple harmonic motion is:

$$T = 2\pi \sqrt{\frac{L}{g}} \quad [2.4]$$

, which proves that the period of oscillation of a simple pendulum is independent of its mass.

## 2.2 Pendulum motion

In order to model the system, an equation needs to be derived that describes the motion of a pendulum bob. This equation will provide displacement and velocity values at discrete time intervals. There are two cases to consider, when the system is with or without damping.

According to Charalambides M. (2001), the equation describing any pendulum in the undamped system is:

$$mx'' + \left(\frac{mg}{L}\right)x = 0 \quad [2.5]$$

and the equivalent for the damped system is:

$$mx'' + cx' + \left(\frac{mg}{L}\right)x = 0 \quad [2.6]$$

, where  $c$  is the damping factor (always positive). By the term damping, we mean that the amplitude of vibration of the oscillatory pendulum becomes progressively smaller. This decrease in amplitude occurs because some of the energy of the oscillating system is used to overcome resistive forces.

## 2.3 Motion of the wall

The equation that describes the displacement of the wall is:

$$x = a \sin \Omega t \quad [2.7]$$

, where  $a$  is the amplitude and  $\Omega$  the angular frequency of the oscillation. The equation describing the velocity is required as well. This is given by the derivative of  $a \sin \Omega t$ , which is:

$$a\Omega \cos \Omega t \quad [2.8]$$

With these two equations the motion of the wall can be modeled and the displacement-velocity parameters can be calculated at discrete time intervals.

## 2.4 Pendulum collisions

When considering a system of more than one pendulum present, we have to investigate the possible case of a collision. For the purpose of this task only elastic collisions will be considered, in which there is no loss of kinetic energy.

Suppose that two particles,  $A$  and  $B$  with

masses  $m_1$  and  $m_2$  respectively, that move in the same straight line, are involved in a collision. Assume that just before the collision, particle  $A$  has velocity  $v_1$  and particle  $B$  has velocity  $v_2$  (Fig. 3). The aim is to find the velocity of the particles just after the collision.

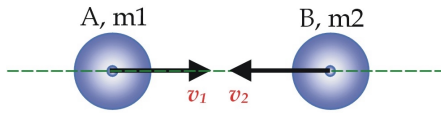


Figure 3. Head-on collision of two particles

To achieve this, we use two fundamental principles of physics. Let the velocities of the two particles after the collision be  $v_1'$  and  $v_2'$  for particles  $A$  and  $B$  respectively. Applying the principle of conservation of energy:

$$\frac{1}{2}m_1v_1^2 + \frac{1}{2}m_2v_2^2 = \frac{1}{2}m_1v_1'^2 + \frac{1}{2}m_2v_2'^2 \quad [2.9]$$

Principle of conservation of linear momentum:

$$m_1v_1 + m_2v_2 = m_1v_1' + m_2v_2' \quad [2.10]$$

Assuming that the masses are identical and solving the above equations, we get:

$$v_1' = v_2 \quad [2.11]$$

$$v_2' = v_1 \quad [2.12]$$

The results show that for the elastic collision there is exchange of velocities.

### 2.5 A system which is driven by a wall

As a means of providing energy, a wall is introduced in the system. The position of the wall is at the left of the first pendulum and its motion is sinusoidal. Furthermore, it has the property of not changing its velocity upon collision because of its mass being much greater than the mass of the pendulum. The aim now is to find an expression for the velocity of the first pendulum after a collision with the wall.

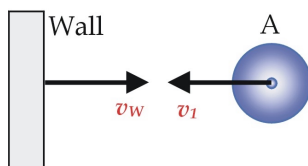


Figure 4. Wall driving the system

Suppose that just before the impact, the wall is

moving with velocity  $v_w$  and the pendulum has a velocity  $v_1$ , in the opposite direction as in figure 4. The relative velocity before the impact is:

$$v_r = v_w - (-v_1) \quad [2.13]$$

The relative velocity of the two bodies after the impact, is opposite of the relative velocity before the impact. This means that after the impact:

$$-v_r = v_w - v_1 \quad [2.14]$$

Giving the velocity of the pendulum after the collision as:

$$v_1' = v_w + v_r \quad [2.15]$$

### 3 Procedure

According to Stummel F. and Hainer K. (1980), numerical analysis deals with methods of solving the typical, fundamental mathematical problems encountered in the various fields in which mathematics is applied in practice. These methods can approximate the solution of differential equations when this is difficult or impossible to be achieved analytically.

As suggested by equation [2.6], all the pendula of the system are described by the same second-order differential equation. The aim is to solve these equations and obtain displacement as well as velocity values at discrete time intervals. One way to go about the problem is to solve the equations analytically, but a more efficient approach is to use certain algorithms that can approximate the solution of a differential equation (numerical solution). One such algorithm is the Runge-Kutta-Nystrom method (Kreyszig E. 1993), which was used in the simulations (Appendix 1).

According to Baker G.L. and Gollub J.P. (1992), 'chaos' is the irregular and unpredictable time evolution of many non-linear systems. For the system under consideration, the motion of the pendula is described by second order linear differential equations, whereas the motion of the wall is described by non-linear equations. Further non-linearity is introduced by the collisions that cause sudden changes in the dynamical variables describing the properties of the system – for example position and velocity of the pendula.

Several analytical and computational tools were utilized as to study the chaotic nature of the system. These include Poincaré sections, return maps (mean position and collision return maps) as well as bifurcation diagrams. Plots concerning these tools are presented in the next section.

## 4 Simulation Results

The simulations were performed on SUN Sparc processors. The differential equation that was numerically solved is:

$$x''+cx'+gx=0$$

, with  $c$  representing the damping factor and  $g$  the constant number 9.80665 (gravitational acceleration). At this point a new notation is adopted, the frequency ratio  $R$ . This is the ratio between the wall angular frequency ( $\Omega$ ) and the natural frequency of the pendulum ( $\omega$ ), given by:

$$R=\frac{\Omega}{\omega}$$

For the simulations that follow, this ratio is varied (by changing  $\Omega$ ) whereas the damping factor, the wall amplitude and the initial conditions of the pendula are kept constant as follows (unless stated otherwise):

- Damping factor = 0.0001
- Wall amplitude = 1.0001
- All pendula are at rest, located at their mean positions. They are separated by 1m and the first one has an offset of 1m from the wall.

### 4.1 Poincaré section

This simulation concerns a single damped pendulum driven by an oscillating wall, with  $R=1.1$ . The results are graphically presented in figure 5.

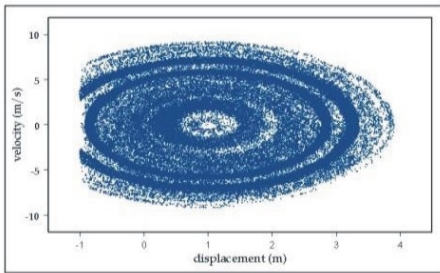


Figure 5. Poincaré section of the single damped driven pendulum ( $R=1.1$ )

The attractor has a circular shape with some areas being denser than others. This means that the pendulum is switching between different energy levels where some of them are visited more frequently than others. Note that the pendulum does not have data points in the area where the displacement is less than  $-1m$ . This is because the displacement cannot be less than the maximum negative displacement of the wall.

The structure of the attractor is fractal since it

shows self-similarity i.e. the inner circular patterns resemble the overall shape. The question is how did this chaotic attractor form? Recall that the Poincaré method is a section through the phase space. The scattered dots were all produced from one trajectory that wanders considerably through the phase space, possibly forming a strangely shaped torus.

With the same frequency ratio, another four pendula are added to the system. The Poincaré section of the 4th pendulum is presented in figure 6.

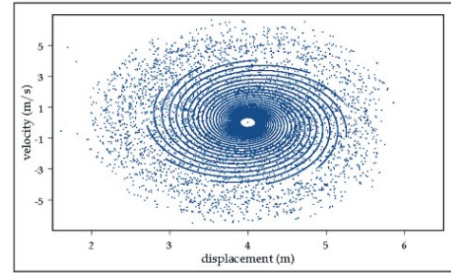


Figure 6. Poincaré section of the 4<sup>th</sup> pendulum ( $R=1.1$ )

The attractor suggests that the pendulum moves both periodically and chaotically. The outer ring is chaotic but as the velocity gets progressively smaller, the motion becomes periodic (well-defined circular lines). Considering that there is damping in the system, the energy provided by the driving force is inversely proportional to the distance away from it. Since the offset of the 4th pendulum is four meters, the long-term amplitude of oscillation is small. This leads to fewer impacts with the other pendula thus making the motion linear. All the data points are drawn towards a point attractor at coordinates (4,0), where the pendulum finally comes to rest.

Plots for the same pendula at a frequency ratio of 1.3 can be found in Appendix 2.

### 4.2 Mean position return map

#### 4.2.1 Frequency ratio = 1.1

Figure 7 is the return map of the single damped driven pendulum. The plot illustrates the presence of both periodic (straight line) as well as chaotic motion. Notice that both axis represent velocities.

The chaotic attractor is very structured with remarkable pattern formation. When part of it is enlarged as shown below, fractal geometry is revealed. The three ellipses are self-repeating and the motion of the data points around them create further boundaries within the attractor. The structure in general is symmetric.

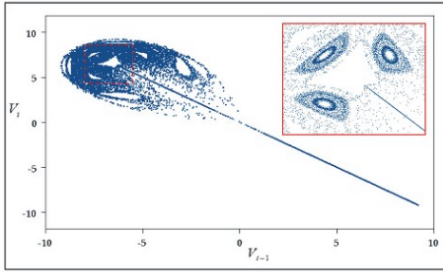


Figure 7. Return map of the single damped driven pendulum ( $R=1.1$ )

We next investigate a system of five pendula driven by an oscillating wall. The formation of two attractors is presented in figure 8. The plot is the return map of the 4th pendulum of the system.

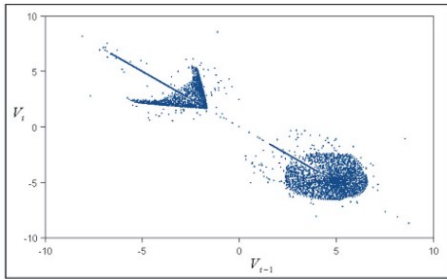


Figure 8. Return map of the 4<sup>th</sup> pendulum ( $R=1.1$ )

#### 4.2.2 Frequency ratio = 1.3

The angular frequency of the driving force is now increased such that the frequency ratio,  $R=1.3$ . Figure 9 is the return map of the single damped driven pendulum.

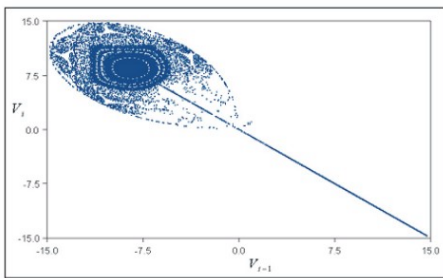


Figure 9. Return map of the single damped driven pendulum ( $R=1.3$ )

The general shape of the chaotic attractor is similar to the previous case when  $R=1.1$ . The internal structure though is very different but still fractal. Notice that the wall now provides the system with more energy, since the velocity range of the pendulum is higher. The same applies to the 4<sup>th</sup> element of a system consisting of five pendula (Fig. 10). There is a change in the attractor shape but it is still chaotic.

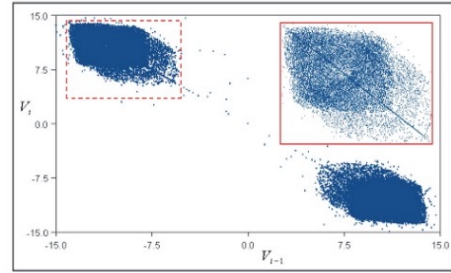


Figure 10. Return map of the 4<sup>th</sup> pendulum ( $R=1.3$ )

### 4.3 Collision return map

#### 4.3.1 Frequency ratio = 1.1

The first case concerns the single damped driven pendulum. Figure 11 represents the pendulum's return map at a frequency ratio,  $R=1.1$ . The attractor is purely chaotic with evident fractal structure. The three dense regions show self-similarity and constitute the overall shape of the attractor.

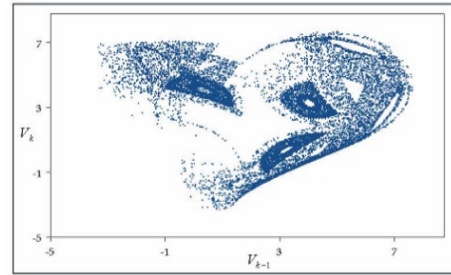


Figure 11. Return map of the single damped driven pendulum ( $R=1.1$ )

The return map of the 4<sup>th</sup> pendulum (colliding with the 3<sup>rd</sup>), in a system of five masses, is presented in figure 12.

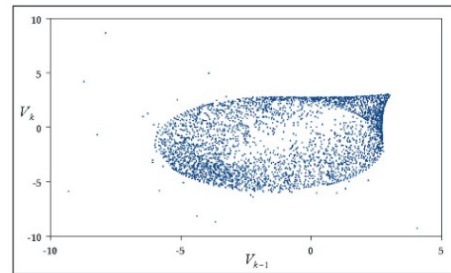


Figure 12. Return map of the 4<sup>th</sup> pendulum ( $R=1.1$ )

The attractor is very similar to the one generated in figure 8 (considering the two attractors joined together).

#### 4.3.2 Frequency ratio = 1.3

The angular frequency of the driving force is now increased such that the frequency ratio,  $R=1.3$ . Figure 13 is the return map of the single damped

driven pendulum. The general attractor shape is similar to the case where  $R=1.1$ , but the internal structure represents a different fractal geometry. The return map of the 4<sup>th</sup> pendulum (colliding with the 3<sup>rd</sup>) in a system of five masses is presented in figure 14.

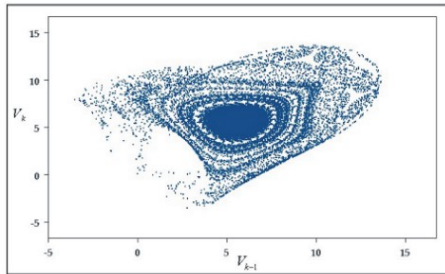


Figure 13. Return map of the single damped driven pendulum ( $R=1.3$ )

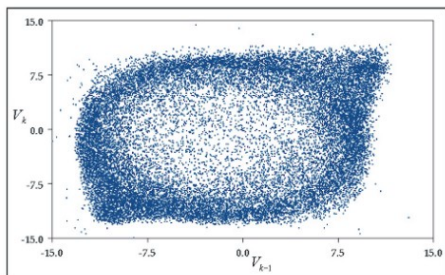


Figure 14. Return map of the 4<sup>th</sup> pendulum ( $R=1.3$ )

After the results presentation of the two types of return maps, there are two points to note. The first one is the relationship between the maps after a small change in the frequency ratio. It is observed that in all cases the overall shape of the attractor remains similar but the internal structure is radically changed. This denotes instability, which is a main characteristic of chaotic systems. The second point is the relationship between the two types of return maps. The results for the same system parameters show that both types produce similar results, or at least similarities in the internal structure of the attractors. A possible explanation would be that a reasonable number of collisions take place close to the mean positions of the pendula.

#### 4.4 Bifurcation diagram

The output of Poincaré section and return maps is based on specific values of the control parameters. To view the dynamics of the system more globally, the amplitude of the driving force is varied and the velocity of a pendulum is observed (Wiggins S. and Stephen 1988).

The system of five driven pendula is examined

at a frequency ratio,  $R=1.1$  and a damping factor of 0.5. The pendula are at rest located at their mean positions and the initial amplitude of the wall is 0.98m, which increments by 0.00005m every 2000 time samples. The bifurcation diagrams of two pendula are examined in the sections that follow.

##### 4.4.1 First pendulum

The bifurcation diagram of the first pendulum is presented in figure 15(a). The results demonstrate both periodic as well as chaotic behaviour. The pendulum starts to oscillate when the amplitude of the wall has increased enough to cause a collision. This occurs at an amplitude of 1m, causing the pendulum to move chaotically. With further amplitude increase, the motion demonstrates periodicity that is described by well-defined lines (at 1.05m). The interchange between the two states occurs repeatedly as the control parameter progresses.

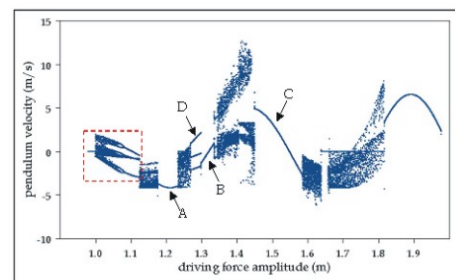


Figure 15(a). Bifurcation diagram of the 1<sup>st</sup> pendulum

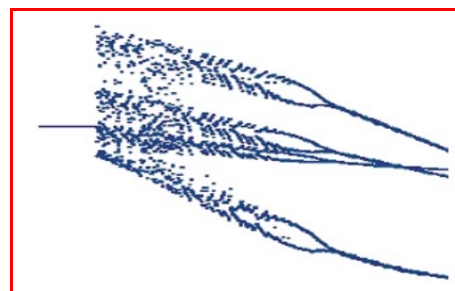


Figure 15(b). Enlarged area

Note that period one is described by a single line (points A-C), while period three by three lines (point D). Usually period multiplication precedes chaotic behaviour, however, for the system under consideration it is usually observed that chaos immediately follows period one. This indicates that the system is very sensitive and the transition between stability and chaos difficult to observe. The enlarged area (Fig. 15(b)) is the only part of the plot that shows a slow and observable transition. One

can observe the transition by examining the plot from right to left. The single lines undergo period doubling. Further splitting leads to chaos.

#### 4.4.2 Third pendulum

Similar results are obtained for the third pendulum (Appendix 3), however the energy associated is lower (smaller range of velocities). Furthermore, it can be observed that the pendulum spends a lot of time at rest. This accounts for the high damping factor employed to the system. But even so, just one impact can drive the body directly from rest to chaos.

Bifurcation diagrams of the same pendula at a frequency ratio  $R=1.2$  can be found in Appendix 4.

### 5 Conclusion

Although our study of Newton's cradle is not a traditional agent-based one, it aims to advance the art of complex systems simulation. The architecture of the system includes a number of co-operating components, with each one performing a specific function as well as providing a clear interface to other components that can utilize its processing capabilities. Two major components are the system controller and the filters. The data generated by the former can be voluminous and the representation not easy to interpret. The filter component is able to manipulate this data according to the investigation requirements of the simulation. This method could be used in classical agent-based modelling to extract only the required elements for analysis.

In the process of simulating the system, initial consideration was given to the single driven pendulum. The results illustrated chaotic attractors with remarkable fractal geometry. Pattern formation and self-similarity were apparent. For the five-pendulum system some results were periodic while others chaotic, depending on the initial conditions and the pendulum under consideration. The return maps indicated that the chaotic motion of neighbouring pendula was correlated. This led to the investigation of spatio-temporal chaos. Observing the Poincaré sections and return maps for different frequency ratios, one could say that in most cases, pendula in the same system share chaotic attractors of similar geometry. This means that the chaotic motion is correlated from one pendulum to another. For a spatially extended system this is known as spatio-temporal chaos. Note that the greater the number of pendula in the system, the more the degrees of freedom, making the

investigation harder compared to the one-pendulum system. Further work was done with the use of bifurcation diagrams. Their results demonstrated that the system can behave both periodically and chaotically as one of the control parameters is varied.

Considering both one and five pendulum systems, a slight change in the initial conditions altered the structure of the chaotic attractors. This denotes instability, which is one of the main characteristics of chaotic systems. However, the fact that there is pattern formation indicates the existence of order out of chaos.

### 6 References

- Baker G.L. & Gollub J.P. (1992), Chaotic dynamics-An introduction, Cambridge University press.
- Charalambides M. (2001), Newton's cradle simulator, B.Sc. (Hons) thesis, University of Surrey, Guildford.
- Devaney R.L. (1992), Chaotic dynamical systems, Addison Wesley.
- Kreyszig E. (1993), Advanced engineering mathematics, 7th edition, John Wiley.
- Muncaster R. (1993), A-Level physics, 4th edition, Stanley Thornes.
- Stummel F. & Hainer K. (1980), Introduction to numerical analysis, Scottish Academic press.
- Wiggins S. & Stephen (1988), Global bifurcations and chaos, Springer-Verlang.

### Appendix 1

The Runge-Kutta-Nystrom algorithm computes the solution of the initial value problem,

$$y'' = f(x, y, y'), y(x_0) = y_0, y'(x_0) = y_0'$$

at equidistant points

$$x_1 = x_0 + h, \quad x_2 = x_0 + 2h, \dots, x_N = x_0 + Nh$$

where  $f$  is such, that this problem has a unique solution of interval  $[x_0, x_N]$ .

INPUT: Initial values  $x_0, y_0, y_0'$ , step size  $h$ , number of steps  $N$

OUTPUT: Approximation  $y_{n+1}$  to the solution  $y(x_{n+1})$  at  $x_{n+1} = x_0 + (n+1)h$ , where  $n=0, 1, \dots, N-1$

For  $n = 0, 1, \dots, N - 1$  do:

$$k_1 = \frac{1}{2} hf(x_n, y_n, y_n')$$

$$k_2 = \frac{1}{2} hf(x_n + \frac{1}{2}h, y_n + K, y_n' + k_1)$$

where  $K = \frac{1}{2}h(y_n' + \frac{1}{2}k_1)$

$$k_3 = \frac{1}{2} hf(x_n + \frac{1}{2}h, y_n + K, y_n' + k_2)$$

$$k_4 = \frac{1}{2} hf(x_n + h, y_n + L, y_n' + 2k_3)$$

where  $L = \frac{1}{2}h(y_n' + k_3)$

$$x_{n+1} = x_n + h$$

$$y_{n+1} = y_n + h(y_n' + \frac{1}{3}(k_1 + k_2 + k_3))$$

OUTPUT  $x_{n+1}, y_{n+1}$   
 [Approximation to the solution at  $x_{n+1}$ ]

$$y_{n+1}' = y_n' + \frac{1}{3}(k_1 + 2k_2 + 2k_3 + k_4)$$

[Auxiliary value needed for next step]

End Loop

This is a fourth order Runge-Kutta and requires four gradient or "k" terms to calculate  $y_{n+1}$ .

## Appendix 2

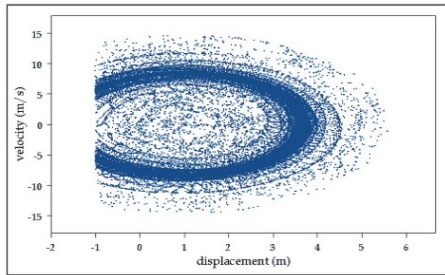


Figure A1. Poincaré section of the single damped driven pendulum (R=1.3)

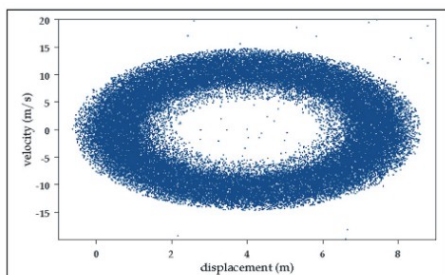


Figure A2. Poincaré section of the 4<sup>th</sup> pendulum (R=1.3)

## Appendix 3

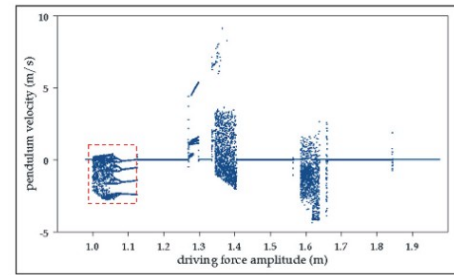


Figure A3(a). Bifurcation diagram of the 3<sup>rd</sup> pendulum

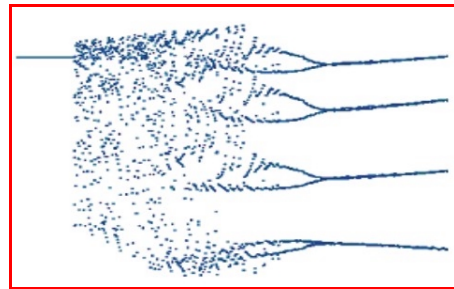


Figure A3(b). Enlarged area

## Appendix 4

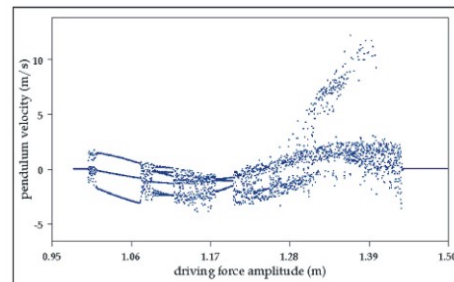


Figure A4. Bifurcation diagram of the 1<sup>st</sup> pendulum (R=1.2)

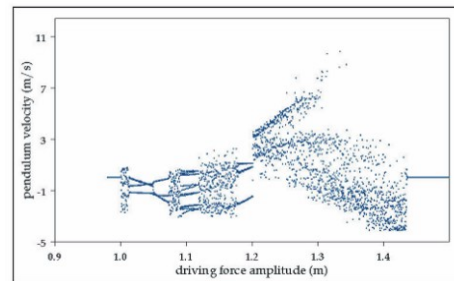


Figure A5. Bifurcation diagram of the 3<sup>rd</sup> pendulum (R=1.2)